

# On Application of Fractal Analysis to Cranial Sutures

Andrzej Z. Górski\*

*Institute of Nuclear Physics,  
Polish Academy of Sciences,  
Cracow, Poland*

Janusz Skrzat†

*Dept. of Anatomy, Collegium Medicum,  
Jagiellonian University,  
Cracow, Poland*

(Dated: November 21, 2018)

## Abstract

Fractal exponents ( $d$ ) for human cranial sutures are calculated using the box counting method. The results were found around  $d = 1.5$  (within the range  $1.3 \div 1.7$ ), supporting the random walk model for the suture formation process. However, the calculated dispersion above the estimated accuracy suggests that other mechanisms are also present. Similar numbers were obtained for both the sagittal and coronal sutures, with the coronal sutures displaying a better scaling. Our results are compared with estimations published by other authors.

PACS numbers: 05.45Df,47.53+n,87.75-k,87.18La

---

\*Electronic address: Andrzej.Gorski@ifj.edu.pl

†Electronic address: jskrzat@poczta.onet.pl

## I. INTRODUCTION

Geometry of a physical object is often characterized by its fractal dimension [1, 2, 3]. This is an adequate description of self-similar sets widely used in various applications, ranging from high energy [4] and condensed matter physics [5] to astrophysics [6] and econophysics [7]. Fractal properties of an object impose strong conditions upon its structure and, in particular, upon a scaling symmetry that is difficult to overestimate in physical applications. It is also a method for quantifying and comparing the spatial complexity of real objects, characteristic of the image as a function of scale. This seems to be especially well suited for morphological analysis. These properties can be used for classification, as well as they should be taken into account in models of morphogenesis.

In this paper, we estimate the fractal dimension of the human cranial sutures. In recent years there were several attempts in this direction [8, 9, 10, 11, 12]. However, to determine the fractal dimension the authors have used an automated commercial software and the obtained values were highly dispersed, the results ranging from 1.0 up to over 1.7. In some cases, rather unphysical results in the range  $0.0 \div 1.0$  were also reported [12] — the cranial suture is a curve and its fractal dimension must be within the range  $1.0 \div 2.0$ . Similar confusions occur also in other areas where a fractal dimension was estimated [13].

In our analysis, we point out the subtleties in determining the fractal dimension that are immanent for such numerical estimates, especially for a relatively limited number of data points, as is in our case. In particular, the crucial point in extracting the fractal dimension from a typical log–log plot is the proper choice of points that are used to get the linear fit. These points should be taken from the scaling region in order to avoid boundary effects that are usually stronger for not very large data sets. Hence, this task should not be left to the automated procedures. Instead, one should perform a careful analysis which points are to be chosen. It will be shown that the standard deviations in the least square fits for two different choices of fitted points can be very small but, in spite of that, both fits lead to considerably different results. Finally, we try to estimate the accuracy of our calculations.

## II. COLLECTING THE DATA

The skulls are stored at the Department of Anatomy of Collegium Medicum of Jagiellonian University. They belong to adult individuals of different sex and derived from different populations. The investigated cranial set presents considerable morphological variation caused by diversified ethnicity and historical dating. Hence, we can expect relatively large standard deviation of calculated fractal exponents for different skulls.

The numerical data have been collected from forty cranial sutures of two types: twenty sagittal and twenty coronal ones. Seventeen of them are from the same skulls and in the last three cases the two types of sutures come from different skulls (to have sutures of better quality). All examined sutures were non-obiterated and their contours were well visible. The segments of the coronal and sagittal sutures, which were visible in superior aspect of the cranial vault, were photographed using the digital camera. The images have sufficient resolution, above 0.1 mm; a sample image for the sagittal suture 03s is displayed in Fig. 1. From these images, using Micrografx Picture Publisher software we extracted one-pixel line being the sutural contour. The pixels were converted into the numbers (2-dimensional coordinates) that were directly used to calculate the fractal dimensions.

We estimate the final accuracy (taking into account details of the suture border) within

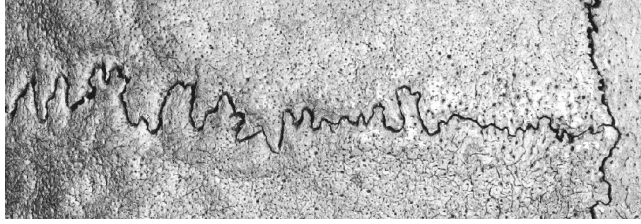


FIG. 1: Sagittal suture 03s.

the range between 0.1 and 0.5 mm, similarly as the other authors [8, 11], while the size of the whole sample is of order 100 mm. *i.e.*, up to about three orders of magnitude. The resulting maximum number of fitted points in the log–log plot should be less than eight. This implies that the expected scaling cannot extend above the range of two orders of magnitude.

We have assumed that the sutures are basically 2-dimensional objects, as the skull’s surface is relatively smooth and the fractal dimensions of sets should be invariant with respect to their smooth transformations. Hence, the numerical data can be viewed as a local projection of sutures to the  $xy$ -plain. As a result, the initial numerical data are sets of the coordinates  $(x, y)$ . The number of data points ( $n_{tot}$ ) in each set varies within the interval  $9\,000 \div 29\,000$ , with the average of above 16 000. For 2-dimensional sets, this is not a very large number and determination of the best fit in the log–log plot should be performed very carefully.

### III. THE BOX COUNTING ALGORITHM

To determine the fractal properties of our data we use the standard box counting algorithm for sets embedded in 2-dimensional plain. The generalized Renyi exponents,  $d_q$ , are defined by [2]

$$d_q = \frac{1}{1-q} \lim_{N \rightarrow \infty} \frac{\ln \sum_i p_i^q(N)}{\ln N} = \lim_{N \rightarrow \infty} \frac{\ln Y_q(N)}{\ln N}, \quad (1)$$

where  $N$  is the number of successive division of a plain into squares (“boxes”),  $p_i(N)$  denote the fractions of the data contained in the  $i$ th box of a given division ( $N$ ), and  $Y_q(N)$  is defined by the second equality. The box size,  $\epsilon \sim 1/N$ . The value of  $d_q$  can be extracted from the log–log plot of the value  $Y_q(N)$  vs  $N$ .

Clearly, for any data set, whether fractal or not, we get the first point ( $N = 1$ ) in the log–log plot with coordinates  $(0, 0)$  ( $p_1(1) = 1$ ). In addition, for any “practical” (finite) set with large enough  $N$ , the value of  $Y_q(N) \rightarrow n_{tot}$  ( $N \rightarrow \infty$ ), where  $n_{tot}$  is the total number of data points (the division becomes so fine that each data point occupies a separate box). In both these regions (too small and too large  $N$ ) the boundary effects become dominant and they are not credible to get an estimate for the fractal dimensions. Hence, one should have a large enough data set to obtain reliable results (sufficient number of fitted points), though the standard fit measures like  $\chi^2$  or Pearson’s  $r$ -coefficient, may look satisfying. This is the main reason why the whole procedure is rather subtle and can give misleading results. Hence, we have used our dedicated box counting code instead of a commercial software to be able to control the intermediate steps.

In our case, the number of points in the log–log plot that is within the reasonable scaling range (linear scaling) equals  $5 \div 7$  — for all plots we repeat calculations for all these three

cases (5, 6 and 7 points) to see differences. The first point we take into account is  $N = 3$  (the box size is  $\frac{1}{8}$  *i.e.*, of order of 1 cm). The upper limit is restricted by the sample size. The corresponding log–log plots are of definitely better quality for the coronal sutures. In Fig. 2 we show, as an example, the plot for the sagittal suture 03s, corresponding to the first row in Table I (for the coronal sutures the fits are better). As can be seen from the plot, the saturation of scaling is clearly visible for  $N = 10$ . Taking into account the points from  $N = 3$  up to  $N = 9$ , we have found that the results considerably deviate from the case when the scaling exponents are calculated up to the  $N = 8$  and  $N = 7$  subdivisions. This is consistent with the fact that, in the subdivision with the factor  $2^9 = 512$ , the details well below 0.5 mm became important. The results for the latter two cases are given in Tables I and II.

The best linear fit is reached in the case of 6 points. The  $\chi^2$  parameter (a sum of the squared deviations from the fit) for  $d_0$  was below 0.05 in most cases. Typically, it was much better for the coronal sutures (on average 0.004 and 0.005 for 6-point and 5-point fits, respectively, leading to the expected “theoretical” accuracy of  $d_q$  below 0.01). For the sagittal sutures, the corresponding values are 0.05 and 0.02, which gives uncertainty for  $d_0$  below 0.02. However, as was stated earlier, one should be aware that a high quality of the linear fit does not guarantee a high accuracy for the resulting real fractal exponent:

(i) a proper choice of the points in the log–log plot is very important and is rather difficult to implement for automated algorithms;

(ii) for some pathological data sets one can obtain misleading results due to their pseudofractal nature [14], in spite of excellent numerical scaling;

(iii) the noise level in the data is unknown and we cannot estimate the real error bars for the point in the log–log plot;

To get reliable results we compare the output of our code for the  $d_q$ -exponents for three adjacent choices of linear fits and for four values of the parameter  $q = 0, 1, 2$ , and 4. This has been done to see the resulting differences in the values of the fractal exponents and to check for possible multifractal and pseudofractal effects. Usually this method provides the fractal exponent with the accuracy of about a few percent.

#### IV. NUMERICAL RESULTS

In our case, the data series are of the average length ( $n_{tot}$ ) of 16 400. For such samples, the crude estimate of the standard Gaussian error is of the order of  $1/\sqrt{n_{tot}} \sim 1\%$  *i.e.* about  $\pm 0.01$  for the estimated value of  $d_q$ . This is quite close to the standard deviations for the linear fits. However, taking into account the problem with a choice of the points to be fitted in the log–log plot, the accuracy in this type of calculations can be roughly *estimated* to be about  $\pm 0.05$ , *i.e.*, about a few percent. The accuracy of those calculations is being depreciated with growing value of the parameter  $q$ . While our results for  $q = 0, 1, 2$  (the capacity, information, and correlation dimension) are the same within  $\pm 0.02$ , the calculated values of  $d_q$ , for  $q = 4$ , differ from the lower  $q$ 's (the difference equals about 0.1 and less). Hence, only the former values of the least square fit are presented in Table I and II.

In the first column, the suture code is given. The number denotes the skull and the labels ( $s, c$ ) denote the suture type (sagittal, coronal). In all the cases the points fitted in the log–log plot were located in the interval  $N = 3 \div 8$  (eq. (1)), where the point (0, 0) is assumed to be the first point and the successive subdivisions differ, as usually, by factor two. The corresponding five-point fit is also given in all cases, below the the 6-point fit. This is

TABLE I: The Renyi exponents for the sagittal sutures.

suture	$d_0$	$d_1$	$d_2$	$\chi^2$
03s	1.39	1.40	1.38	0.04
	1.46	1.48	1.46	0.01
04s	1.53	1.53	1.51	0.05
	1.62	1.61	1.58	0.03
06s	1.54	1.55	1.55	0.05
	1.62	1.64	1.63	0.01
10s	1.47	1.48	1.46	0.07
	1.56	1.57	1.56	0.03
14s	1.56	1.56	1.56	0.07
	1.66	1.66	1.63	0.02
16s	1.57	1.57	1.55	0.04
	1.63	1.64	1.63	0.01
17s	1.51	1.50	1.46	0.08
	1.61	1.59	1.55	0.04
18s	1.57	1.59	1.57	0.04
	1.65	1.67	1.66	0.01
19s	1.44	1.47	1.47	0.03
	1.50	1.55	1.54	0.01
20s	1.58	1.61	1.59	0.06
	1.67	1.70	1.69	0.02
22s	1.59	1.61	1.59	0.03
	1.65	1.68	1.67	0.01
23s	1.43	1.46	1.46	0.04
	1.51	1.55	1.54	0.01
24s	1.56	1.55	1.53	0.07
	1.66	1.65	1.62	0.02
25s	1.55	1.56	1.54	0.08
	1.65	1.65	1.63	0.03
27s	1.50	1.52	1.50	0.04
	1.57	1.59	1.58	0.01
28s	1.45	1.47	1.44	0.04
	1.53	1.55	1.53	0.01
30s	1.50	1.52	1.50	0.05
	1.58	1.61	1.59	0.01
01s	1.40	1.43	1.40	0.04
	1.48	1.51	1.49	0.01
21s	1.48	1.51	1.49	0.05
	1.57	1.60	1.59	0.02
26s	1.48	1.50	1.49	0.04
	1.55	1.57	1.56	0.02

to show the differences for the two neighboring fits. The 7-point fit was also done, however the results are not given in the Tables. In the last column, the estimate for the  $\chi^2$  value is given. These calculations clearly shows that:

(A) For the both, coronal and sagittal sutures, the average differences  $|d_0 - d_1|$  and  $|d_1 - d_2|$  are equal to about 0.01, which is negligible in comparison to the estimated accuracy; the same result can be found for 5, 6 and 7-point fits; this suggests a good *monofractal scaling* within the investigated range (two orders of magnitude);

(B) For the difference  $|d_2 - d_4|$ , taking into account all the calculated fits, we get the difference of 0.02 for coronal and of 0.07 for sagittal sutures; *i.e.*, the coronal sutures are less “noisy”; this is partly due to the data series that are by about 15% longer in this case; however, it is possible that this effect is also connected with the better scaling of the coronal data series;

(C) The 5-point fit gives a systematic difference in comparison with the 6-point fit, on average about +0.02 for the coronal and +0.08 for the sagittal sutures; this suggests that we are already approaching the boundary of scaling and this is another indication of the superior scaling for the coronal sutures;

TABLE II: The Renyi exponents for the coronal sutures.

suture	$d_0$	$d_1$	$d_2$	$\chi^2$
03c	1.44	1.45	1.44	0.006
	1.47	1.48	1.47	0.002
04c	1.36	1.37	1.36	0.001
	1.38	1.38	1.38	< 0.001
06c	1.48	1.53	1.54	0.005
	1.49	1.55	1.56	0.001
10c	1.35	1.35	1.35	0.004
	1.37	1.37	1.36	0.003
14c	1.48	1.51	1.53	0.006
	1.51	1.55	1.58	< 0.001
16c	1.62	1.63	1.61	0.008
	1.65	1.68	1.66	< 0.001
17c	1.51	1.53	1.52	0.003
	1.52	1.55	1.55	0.003
18c	1.30	1.30	1.30	0.003
	1.30	1.29	1.29	0.004
19c	1.28	1.29	1.28	0.006
	1.35	1.35	1.34	0.009
20c	1.49	1.51	1.51	0.003
	1.49	1.51	1.52	0.004
22c	1.58	1.61	1.61	0.012
	1.62	1.66	1.67	0.003
23c	1.45	1.47	1.47	0.002
	1.46	1.48	1.48	0.001
24c	1.57	1.62	1.60	0.010
	1.61	1.67	1.66	< 0.001
25c	1.60	1.65	1.67	0.005
	1.63	1.69	1.71	0.001
27c	1.34	1.37	1.37	0.013
	1.33	1.38	1.37	0.017
28c	1.44	1.45	1.43	0.004
	1.46	1.46	1.43	0.002
30c	1.44	1.51	1.52	0.002
	1.45	1.53	1.55	0.002
07c	1.48	1.51	1.52	0.010
	1.51	1.56	1.57	0.030
11c	1.34	1.39	1.39	< 0.001
	1.35	1.39	1.39	< 0.001
13c	1.44	1.52	1.53	0.006
	1.43	1.52	1.54	0.006

(D) The average values for 5-point and 6-point fits to  $d_0$ ,  $d_1$ , and  $d_2$  and the corresponding standard deviations are given in Table III; the values vary in the range  $1.38 \div 1.70$  (sagittal sutures, Table I) and  $1.29 \div 1.71$  (coronal sutures, Table II), the average values are very close to 1.5 with the standard deviation of about 0.1;

(E) The differences between different sutures are larger than the expected accuracy;

(F) the results for the coronal sutures are a few percent lower than these for the sagittal ones; as the difference is comparable with the estimated error, it can be caused by the bigger noise component;

## V. SUMMARY AND CONCLUSIONS

A detailed analysis of fractal properties of the coronal and sagittal sutures has been performed by applying the box counting algorithm for the data series consisting of about 17 000 points. The final values of the Renyi exponents are equal to about 1.55 for sagittal and 1.47 for coronal sutures. The least square fit ( $\chi^2$ ) for all fits is rather good implying the

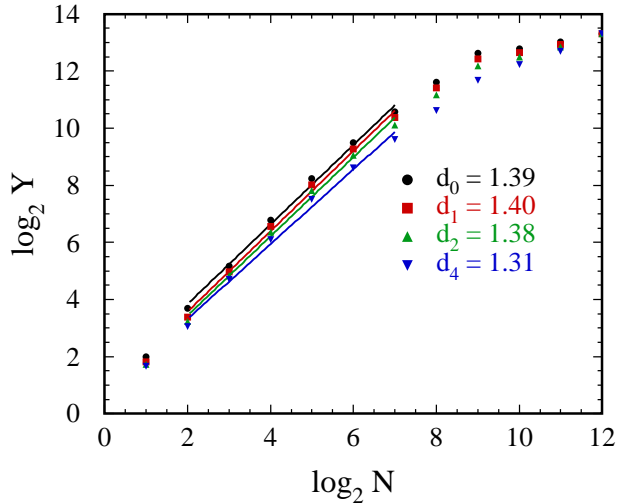


FIG. 2: Example of the log-log plot for the sagittal suture 03s used to extract Renyi exponents in case of 6-point fits. Fits for  $d_q$  with  $q = 0, 1, 2,$  and  $4$  are displayed.

TABLE III: Average values of Renyi exponents.

suture type	fit	$d_0$	$d_1$	$d_2$
sagittal	6-point	1.51	1.52	1.50
sagittal	5-point	1.59	1.60	1.59
total average		1.55	1.56	1.55
coronal	6-point	1.45	1.48	1.48
coronal	5-point	1.47	1.50	1.51
total average		1.46	1.49	1.50

error below  $\pm 0.05$  for the  $d_q$  values, and even lower for the coronal sutures.

We point out that the differences caused by the choice of points to be fitted in the log-log plot lead to higher differences, about 0.10 for the optimal choices:  $N = 3 \div 8$  and  $N = 3 \div 7$ . In our opinion, this is the main source of considerable differences in the results published by other authors (see *e.g.*, Refs. [8, 9, 10, 11, 12]). This applies to other estimates of fractal properties, especially in those cases where the number of data points is relatively modest.

The average value of the fractal exponent for all the sutures taken into account is, within the estimated accuracy, close to 1.5, the exact value for the *Brownian random walk*. This suggests that future models of the suture formation should have the random-walk model as the basic ingredient. For various skulls under investigation, the results differ by up to  $\pm 0.2$ . This indicates that the random walk mechanism, though essential, is not sufficient to explain the suture formation and further investigation is necessary.

---

[1] J. Balatoni and A. Renyi, Publ. Math. Inst. Hung. Acad. Sci **1**, 9 (1956), (in Hungarian); translated in: Selected papers of A. Renyi, vol. 1 (North-Holland Amsterdam 1970).

- [2] A. Renyi, *Probability Theory* (North-Holland, 1970).
- [3] B. B. Mandelbrot, *Fractals: Form, Chance, and Dimension* (Freeman, San Francisco, 1977).
- [4] A. Białas and R. Peszanski, Nucl. Phys. B **308**, 803 (1988).
- [5] D. R. Hofstadter, Phys. Rev. B **14**, 2239 (1976).
- [6] P. H. Coleman, L. Pietronero, and R. H. Sanders, Astron. Astrophys. **200**, L32 (1988).
- [7] A. Z. Górski, S. Drożdż, and J. Speth, Physica A **316**, 496 (2002).
- [8] W. C. Hartwig, J. Morphol. **210**, 289 (1991).
- [9] J. Skrzat, D. Chmiel, and M. Usarz, Medical Review **3**, 418 (2000).
- [10] J. Skrzat and J. Walocha, Folia Morphol. (Warsz) **62**, 119 (2003).
- [11] C. Y. Jack, R. L. Wright, M. Williamson, J. P. Braselton, and M. L. Abell, Cleft Palate–Craniofacial J. **40**, 409 (2003).
- [12] N. Lynnerup and C. B. Jacobsen, Am. J. Phys. Anthropol. **121**, 332 (2003).
- [13] A. Z. Górski, *Comment on fractality of quantum mechanical energy spectra* (1998), [chao-dyn/9804034](#); A. Saiz and V. J. Martínez, Phys. Rev. E **60** (1999) 4993.
- [14] A. Z. Górski, J. Phys. A **34**, 7933 (2001).